RESEARCH ARTICLE

Influence of land-use intensity on the spatial distribution of N-cycling microorganisms in grassland soils

Daniel Keil[1], Annabel Meyer[2], Doreen Berner[1], Christian Poll[1], André Schützenmeister[3], Hans-Peter Piepho[3], Anna Vlasenko[4], Laurent Philippot[5,6], Michael Schloter[2,7], Ellen Kandeler[1] & Sven Marhan[1]

[1]Institute of Soil Science and Land Evaluation, Soil Biology Section, University of Hohenheim, Stuttgart, Germany; [2]Technical University of Munich, Neuherberg, Germany; [3]Institute of Crop Science, Bioinformatics Unit, University of Hohenheim, Stuttgart, Germany; [4]Faculty of Soil Science, Lomonosov Moscow State University, Leninskie Gory, Moscow, Russia; [5]INRA, UMR 1229, Soil and Environmental Microbiology, Dijon, France; [6]University of Burgundy, UMR 1229, Dijon, France; and [7]Terrestrial Ecogenetics Department, Institute of Terrestrial Ecogenetics, Helmholtz Zentrum München, Neuherberg, Germany

Correspondence: Sven Marhan, Institute of Soil Science and Land Evaluation, Soil Biology Section, University of Hohenheim, Emil-Wolff-Strasse 27, 70599 Stuttgart, Germany.
Tel.: +49 711 459 22614;
fax: +49 711 459 23117;
e-mail: sven.marhan@uni-hohenheim.de

Received 24 November 2010; revised 28 February 2011; accepted 5 March 2011.
Final version published online 15 April 2011.

DOI:10.1111/j.1574-6941.2011.01091.x

Editor: Riks Laanbroek

Keywords
grassland; land-use intensity; ammonia oxidizers; denitrifiers; geostatistics.

Abstract

A geostatistical approach using replicated grassland sites (10 m × 10 m) was applied to investigate the influence of grassland management, i.e. unfertilized pastures and fertilized mown meadows representing low and high land-use intensity (LUI), on soil biogeochemical properties and spatial distributions of ammonia-oxidizing and denitrifying microorganisms in soil. Spatial autocorrelations of the different N-cycling communities ranged between 1.4 and 7.6 m for ammonia oxidizers and from 0.3 m for *nosZ*-type denitrifiers to scales > 14 m for *nirK*-type denitrifiers. The spatial heterogeneity of ammonia oxidizers and *nirS*-type denitrifiers increased in high LUI, but decreased for biogeochemical properties, suggesting that biotic and/or abiotic factors other than those measured are driving the spatial distribution of these microorganisms at the plot scale. Furthermore, ammonia oxidizers (*amoA* ammonia-oxidizing archaea and *amoA* ammonia-oxidizing bacteria) and nitrate reducers (*napA* and *narG*) showed spatial coexistence, whereas niche partitioning was found between *nirK*- and *nirS*-type denitrifiers. Together, our results indicate that spatial analysis is a useful tool to characterize the distribution of different functional microbial guilds with respect to soil biogeochemical properties and land-use management. In addition, spatial analyses allowed us to identify distinct distribution ranges indicating the coexistence or niche partitioning of N-cycling communities in grassland soil.

Introduction

The characterization of spatial patterns of microorganisms in terrestrial ecosystems is important in order to understand the underlying factors and soil properties controlling their distribution and hence their importance in ecosystem functions (Ettema & Wardle, 2002). Accordingly, the spatial distribution of microorganisms has been investigated in an increasing number of studies in recent years (e.g. Franklin & Mills, 2003; Becker *et al.*, 2006; Miller *et al.*, 2009; Philippot *et al.*, 2009a, b; Bru *et al.*, 2010; Enwall *et al.*, 2010).

The published data are contradictory and depend mainly on the investigated scale. For example Franklin & Mills (2003) postulated that bacterial distribution patterns can be highly structured, even within a habitat that appears to be relatively homogeneous at the plot and field scale. At larger scales, however, Fierer & Jackson (2006) reported microbial biogeography as spatially independent at continental scales.

Grassland soils are of special interest in studying the spatial distribution of microbial communities because of the strong relationships between plants and microorganisms (Niklaus *et al.*, 2006; Bremer *et al.*, 2007) and the heterogeneous influence of grazers on soil properties (Bardgett & Wardle, 2003). Indeed, Ritz *et al.* (2004) reported that the spatial distribution of microbial communities was influenced by soil nutrient status. Similarly, the spatial distribution of several bacterial phyla in a pasture was correlated to soil properties such as pH, soil moisture or ammonium and nitrate concentration (Philippot *et al.*, 2009a). These studies investigating the spatial distribution of microorganisms in

grassland soil have mostly focused on total microbial communities. However, both herbivores and fertilization regimes have been shown to affect N-cycling and the corresponding microbial communities in grassland soils (Frank & Groffmann, 1998; Le Roux *et al.*, 2003; Patra *et al.*, 2005). Within the N-cycle, nitrifying and denitrifying communities are responsible for N-losses through nitrate (NO_3^-) leaching or greenhouse gas emissions in the form of nitrous oxide (N_2O) (Philippot *et al.*, 2007). The first step in nitrification, the aerobic oxidation of ammonium (NH_4^+) to nitrite (NO_2^-), can be performed by both archaea and *Proteobacteria* having *amoA* ammonia-oxidizing archaea (AOA) or *amoA* ammonia-oxidizing bacteria (AOB) genes, respectively (Rotthauwe *et al.*, 1997; Treusch *et al.*, 2005). Denitrification, the anaerobic reduction of NO_3^- to NO_2^- and to the gaseous N species NO, N_2O and N_2, is performed by a more diverse group of bacteria and archaea (Tiedje *et al.*, 1989; Zumft, 1997; Philippot, 2002). The spatial distributions of nitrifying and denitrifying microorganisms have been investigated at scales ranging from millimeters (Grundmann & Debouzie, 2000) to the landscape level (Bru *et al.*, 2010). A recent study of Enwall *et al.* (2010), exploring the spatial patterns of community structure, size and activity of denitrifying bacteria in both an integrated and an organic crop production system, again underlined the role of soil properties in shaping denitrifying communities. Differential habitat selection was observed for the denitrifiers having the NirS- and NirK-type nitrite reductases, with copper being a stronger driver of the abundance of the *nirK*- than *nirS*-type denitrifiers, while soil nitrate and clay were unique drivers for the *nirS* denitrifier community structure. These results suggested niche differentiation between denitrifiers having the two types of nitrite reductases to avoid competitive exclusion.

Although published data clearly indicate the role of plant community composition as well as soil properties as drivers for microbial distribution patterns in soil, little is known about the extent to which the land-use intensity (LUI) of grasslands influences the spatial distribution of microbial communities involved in N-cycling. For grazed grassland ecosystems, Ritz *et al.* (2004) showed that the intensity of land use, such as the application of fertilizer, affected soil properties and subsequently plant species composition and diversity of soil microorganisms. More recently, Philippot *et al.* (2009b) found that the intensity of cattle grazing together with soil properties strongly affected the spatial patterns of both the relative abundance and the activity of denitrifying bacteria. The studies mentioned above were conducted on a single site per treatment only. In order to investigate whether the spatial distribution of microbial communities is significantly affected by grassland management, a geostatistical approach on replicated sites is needed.

The objective of this study, therefore, was to investigate whether LUI changes the spatial distribution of microorganisms involved in nitrogen cycling at the plot scale ($10\,m \times 10\,m$) using replicated grassland sites subjected either to low (unfertilized pastures with sheep grazing) or to high LUI (fertilized meadows, mown 2–3 times per year). We hypothesized that management practices such as fertilizer application and mowing at high LUI sites result in reduced spatial heterogeneity of soil biogeochemical properties and subsequently reduced spatial heterogeneity of microorganisms in comparison with grassland sites of low LUI. We assessed the abundances of total bacterial genes (16S rRNA gene), archaeal and bacterial ammonia oxidizers (*amoA* AOA, *amoA* AOB) and denitrifiers (*napA*, *narG*, *nirK*, *nirS* and *nosZ*) using quantitative real-time PCR (qPCR). In addition, soil biogeochemical properties potentially controlling microbial abundance were determined. Data were analyzed using a linear mixed model approach with a geostatistical covariance structure. Ordinary kriging was used to map the spatial distribution of ammonia-oxidizing and denitrifying communities of the study sites.

Materials and methods

Study site

The sites investigated in this study are located in a limestone middle mountain range, the UNESCO Biosphere region 'Schwäbische Alb' in Southwestern Germany. The climate is moderate, with an average annual precipitation of 700–1000 mm a^{-1} and mean annual temperatures of 6–7 °C. Sites are located between 690 and 810 m above sea level. Soil at the sites is identified as Rendzic Leptosol. An overview of the sites is presented in Table 1. We investigated six grassland sites at two different land-use intensities: (1) unfertilized pastures (low LUI) and (2) fertilized meadows that are mown 2–3 times per year (high LUI). These sites are part of the 'German Biodiversity Exploratories' and have been named as AEG 1–3 (high LUI) and AEG 7–9 (low LUI) (Fischer *et al.*, 2010).

Soil sampling

Sampling took place in spring (April, 2008), before the beginning of active plant growth. At each of the six grassland sites, bulk soil cores from 0 to 10 cm depth were taken using core augers (Ø 58 mm), and surface vegetation was removed. Samples were collected from a total area of 10×10 m per site. A grid mesh with 2.5 m distances was laid over each of the six sites and soil samples were taken starting at each grid point (Supporting Information, Fig. S1). Spatially randomized sampling distances, starting from each grid point and diminishing from 150, 100, 50, 25 to 12.5 cm, resulted in 54 soil cores per site for laboratory

Table 1. Site description

LUI	Site ID	Management type	Plant diversity (number of vascular species)*	Altitude a.s.l. (m)	Latitude	Longitude
Low	AEG 7	Unfertilized pasture, sheep	46	795	48°23′29″N	9°22′37″E
	AEG 8	Unfertilized pasture, sheep	43	760	48°25′22″N	9°29′32″E
	AEG 9	Unfertilized pasture, sheep	58	745	48°23′41″N	9°30′10″E
High	AEG 1	Fertilized meadow, mown two times	26	690	48°23′53″N	9°20′31″E
	AEG 2	Fertilized meadow, mown three times	17	750	48°22′37″N	9°28′22″E
	AEG 3	Fertilized meadow, mown two times	28	810	48°24′32″N	9°31′57″E

*A. Meyer, pers. commun.

analyses. An additional sample directly adjacent to each soil core was collected to determine bulk density. Soil cores were packed in plastic bags and stored at $-24\,^{\circ}C$ for further analysis. Before analyses, roots, stones and soil macrofauna were removed, and soils were sieved (< 5 mm) and homogenized.

Soil biogeochemical properties

Soil pH was determined in 0.01 M $CaCl_2$ [soil to solution ratio (w/v) 1 : 2.5]. The soil water content (SWC, expressed as % soil dry weight) was determined gravimetrically for each sample after drying at 105 °C for 24 h. Soil organic C (C_{org}) and total N (N_t) contents were measured using an elemental analyzer (Leco C/N 2000, Leco Corporation, St. Joseph). Ammonium (NH_4^+) and nitrate (NO_3^-) were extracted with 1 M KCl [soil to extractant ratio (w/v) of 1 : 4], shaken on a horizontal shaker for 30 min at 250 r.p.m. and centrifuged for 30 min at 4400 ***g***. The concentrations of NH_4^+ and NO_3^- were measured on an autoanalyzer (Bran & Luebbe, Norderstedt, Germany). Soil microbial biomass carbon (C_{mic}) and nitrogen (N_{mic}) were determined using the chloroform fumigation extraction method (Vance *et al.*, 1987) in 5 g soil subsamples and extracted with 20 mL 0.5 M K_2SO_4 on a horizontal shaker for 30 min at 250 r.p.m. and centrifuged for 30 min at 4400 ***g***. A second sample remained nonfumigated, but was treated identically otherwise. C and N in supernatants were measured on a Dimatoc 100 DOC/TN-analyzer (Dimatec, Essen, Germany) and C_{mic} and N_{mic} were estimated using the conversion factors 0.45 (Joergensen, 1996) and 0.54 (Joergensen & Müller, 1996), respectively. Extractable organic C (EOC) and N (EN) were calculated from the C and N concentrations in the supernatants of the nonfumigated samples.

DNA extraction

DNA was extracted from a homogenized soil subsample (0.2 g) using the FastDNA® SPIN for Soil Kit (MP Biomedicals, LLC, Solon, OH) according to the manufacturer's instructions. Quantification and quality evaluation of the extracted DNA were specified using the NanoDrop® ND-1000 spectrophotometer (Thermo Fisher Scientific, Waltham, MA).

qPCR assays

qPCR was applied to assess the abundance of 16S rRNA genes as a proxy for the total bacterial community, the ammonia-oxidizing community by targeting genes encoding the catalytic subunits of archaeal and bacterial ammonia monooxygenase enzymes (*amoA* AOA and *amoA* AOB) and the denitrifier community by quantification of genes encoding the catalytic subunits of enzymes involved in the denitrification pathway (*napA*, *narG*, *nirK*, *nirS* and *nosZ*). PCR reactions were performed according to published protocols. Details are given in Table 2. For all qPCRs, before the experiments, optimal dilutions were tested to avoid the inhibitory effects of coextracted humic acids and other substances.

Statistical analyses

For a realistic estimation of soil biogeochemical properties in terms of geostatistical analyses and microbial abundances, all data were expressed on an area basis of soil for the top 10 cm soil layer (m^{-2}) (Bolton *et al.*, 1990, 1993; Doran & Parkin, 1996). Geostatistical analyses were performed to interpret the spatial distribution of environmental properties as well as the abundance of ammonia oxidizers and denitrifiers in soil. We analyzed 18 different soil chemical and microbial parameters in total. Differences in heterogeneity among the two LUIs according to the above parameters were investigated by fitting two linear mixed models with geostatistical covariance. The full linear mixed model that we considered fits a separate spatial covariance structure to each level of LUI, i.e. a separate nugget effect, a separate sill and separate range. Thus, there are three additional parameters fitted compared with the reduced model. We used a restricted maximum likelihood approach to fit both mixed models. The fixed effect part of both mixed models is equal. We were therefore able to use a *likelihood ratio test* (LRT) to infer whether the covariance structure of the full model fitted significantly better than the reduced model (Schabenberger & Pierce, 2002).

Table 2. Conditions and protocols used in qPCR

Gene	Primer	Reference	Source of standard	Thermal profile	No. of cycles	Efficiency mean (%)	Primer (μM)	Template (ng)	Supplement	PCR machine*
16S rRNA gene	341F 534R	López-Gutiérrez *et al*. (2004)	*Pseudomonas aeruginosa* PAO1	95 °C – 15 s, 60 °C – 30 s, 72 °C – 30 s	35	104	2	7.5	T4gp32 (100ng)	ABI 7500 Fast Real-Time PCR
amoA AOA	19F CrenamoA 616r48x†	Leininger *et al*. (2006)	Fosmid clone 54d9	94 °C – 45 s, 55 °C – 45 s, 72 °C – 45 s	40	85	2	5	BSA (v/v) 0.06%	ABI 7300 Real-Time PCR
amoA AOB	*amoA* 1F *amoA* 2R	Rotthauwe *et al*. (1997)	*Nitrosomonas* sp.	94 °C – 45 s, 58 °C – 45 s, 72 °C – 45 s	40	90	3	5	BSA (v/v) 0.06%	ABI 7300 Real-Time PCR
napA	*napA* 3F	Bru *et al*. (2007)	*Pseudomonas aeruginosa* PAO1	95 °C – 15 s, 61 °C – 30 s, 72 °C – 30 s	6 (– 1 °C/cycle)	99	2	7.5	T4gp32	ABI 7500 Fast Real-Time PCR
	napA 4R			95 °C – 15 s, 56 °C – 30 s, 72 °C – 30 s, 80 °C – 30 s	35				(100ng)	
narG	*narG*G-F	Bru *et al*. (2007)	*Pseudomonas aeruginosa* PAO1	95 °C – 15 s, 63 °C – 30 s, 72 °C – 30 s	6 (– 1 °C/cycle)	88	2	7.5	T4gp32	ABI 7500 Fast Real-Time PCR
	*narG*G-R			95 °C – 15 s, 58 °C – 30 s, 72 °C – 30 s, 80 °C – 30 s	35				(100ng)	
nirK	*nirK* 876F	Henry *et al*. (2004)	*Sinorhizobium meliloti*	95 °C – 15 s, 63 °C – 30 s, 72 °C – 30 s	6 (– 1 °C/cycle)	108	2	7.5	T4gp32	ABI 7500 Fast Real-Time PCR
	nirK 1040R			95 °C – 15 s, 58 °C – 30 s, 72 °C – 30 s, 80 °C – 30 s	35				(100ng)	
nirS	*nirS* 4QF	Kandeler *et al*. (2006)	*Pseudomonas fluorescens* C7R12	95 °C – 15 s, 63 °C – 30 s, 72 °C – 30	6 (– 1 °C/cycle)	84	2	7.5	T4gp32	ABI 7500 Fast Real-Time PCR
	nirS 6QR			95 °C – 15 s, 58 °C – 30 s, 72 °C – 30 s, 80 °C – 30 s	35				(100ng)	
nosZ	*nosZ* 2F	Henry *et al*. (2006)	*Bradyrhizobium japonicum* USDA 110	95 °C – 15 s, 65 °C – 30, 72 °C – 30 s	6 (– 1 °C/cycle)	103	2	7.5	T4gp32	ABI 7500 Fast Real-Time PCR
	nosZ 2R			95 °C – 15 s, 60 °C – 30 s, 72 °C – 30 s, 81 °C – 30 s	35				(100ng)	

*Applied Biosystems Inc. (Foster City, CA).
†Leininger *et al*. (pers. commun. to A. Meyer).

The linear mixed model for one specific variable can be written as:

$$y_{ijk} = \delta_i + p_{ij} + t_{ijk} + \varepsilon_{ijk}, \quad (1)$$

where y_{ijk} represents the kth measurement of a soil sample coming from the jth grassland site, which was managed at the ith intensity class. The term δ_i references the ith fixed effect for treatment (LUI), p_{ij} represents the ijth random plot effect, which is distributed as $p_{ij} \sim N(0, \sigma_p^2)$, t_{ijk} is the spatial trend effect, and the residual errors terms ε_{ijk} are distributed as $\varepsilon_{ijk} \sim N(0, \sigma_R^2)$. In spatial modeling, the error variance δ_R^2 is usually denoted as a nugget effect. The spatial trend effect t_{ijk} is used to model the covariance of each pair of observations (m, n) with locations (x_m, y_m) and (x_n, y_n) depending on their separation distance

$$h = \sqrt{(x_m - x_n)^2 + (y_m - y_n)^2}. \quad (2)$$

The covariance function can be written as

$$C(h) = \sigma_V^2 \cdot \rho(h), \quad (3)$$

where σ_V^2 denotes the variance parameter, which is usually called the sill or the scale parameter, and $\rho(h)$ corresponds to the correlation function, which determines the spatial dependency among observations as a function of distance h. We considered the Gaussian, exponential and spherical models (Schabenberger & Pierce, 2002) and confined the analysis to that spatial model for which we obtained the best-fitting full model.

We used the statistical software SAS version 9.2, specifically the *MIXED* procedure, to fit both models for each variable. The resulting *P*-values for the LRT were adjusted for multiple testing using the Bonferroni-correction method, which controls the family-wise error rate. It is rather conservative, i.e. differences have to be greater in order to be declared significant (SAS Institute Inc., 1999).

The sampling locations were randomly chosen and revealed a rather coarse picture of the existing conditions regarding a specific variable. In order to smooth the data, we used the covariance parameter estimates obtained from fitting the linear mixed models, and used them as parameters for an *ordinary kriging* (OK) procedure (PROC KRIGE2D of the SAS system), which yielded estimates of $y_{ijk} - e_{ijk}$.

This procedure is equivalent to the best linear unbiased prediction of the same quantity based on mixed model (1) (Robinson, 1991). We used KRIGE2D instead of the MIXED procedure for kriging because of computational speed. The spatial covariance model determines the way in which optimal weights are calculated for kriging (Isaaks & Srivastava, 1989). Spatial dependence and autocorrelation were described by a distinct set of spatial parameters that were estimated for each LUI when the model was able to separate between the two LUI. The ratio of partial sill to total sill (p-Sill/Sill) was expressed as percentage and used to classify spatial dependence. A ratio of $< 25\%$ indicated weak spatial dependence, 25–75% indicated moderate spatial dependence and $> 75\%$ indicated strong spatial dependence (Cambardella *et al.*, 1994). The practical range (p-Range) is expressed in meters and was used as an indicator for the scale of spatial autocorrelation, i.e. high spatial autocorrelations indicate reduced spatial heterogeneity of a certain property at the investigated scale.

Spearman correlations were calculated including both LUIs and separately for low and high LUI to determine pairwise relationships between the parameters. The resulting *P*-values were adjusted for multiple testing using the Bonferroni-correction method as described for the LRT. Both correlation analysis and plotting of kriged maps were performed using the software R (R Development Core Team, 2008), version 2.9.1. To test differences between the two LUI, one-way ANOVA were performed for soil biogeochemical properties and gene abundances with the fixed factor 'LUI' using STATISTICA 6.0 (StatSoft Inc., Tulsa, OK). Transformation of data has been carried out with appropriate means to meet the requirements of a normal distribution and homogeneity of variance if required.

Results

Soil biogeochemical properties

The average values of soil biogeochemical properties for each plot are given in Table S1. Bulk densities ranged from 0.64 to 0.83 g soil dry weight cm^{-3}, with both minimum and maximum values found in low LUI sites, and soil pH values ranged from 6.4 to 7.1. SWC did not significantly differ between low and high LUI ($P = 0.878$). Neither bulk density nor pH differed significantly between the two LUI. In high LUI, total nitrogen tended to be higher ($P = 0.088$) and NO_3^- amounts were significantly higher ($P = 0.023$), while C_{mic} was significantly higher ($P = 0.029$) and N_{mic} tended to be higher ($P = 0.081$) in the high LUI sites.

Abundances of total bacteria, ammonia oxidizers and denitrifiers

Bacterial 16S rRNA gene copy numbers, which were used as a proxy for estimating the number of total bacteria, ranged between 5.8×10^{15} and 1.7×10^{16} copies m^{-2} (Fig. 1) (equivalent to 9.5×10^9 and 2.1×10^{10} copies g^{-1} dry soil, Table S2). Comparison of the abundance of total bacteria between LUIs using the data expressed on an area basis did not show any significant differences (Fig. 1). In contrast, AOA had a significantly higher abundance ($P = 0.022$) in the high LUI sites (Fig. 1). The same trend was observed for AOB, but the difference was not significant ($P = 0.065$). Among the denitrification genes, LUI had a significant effect

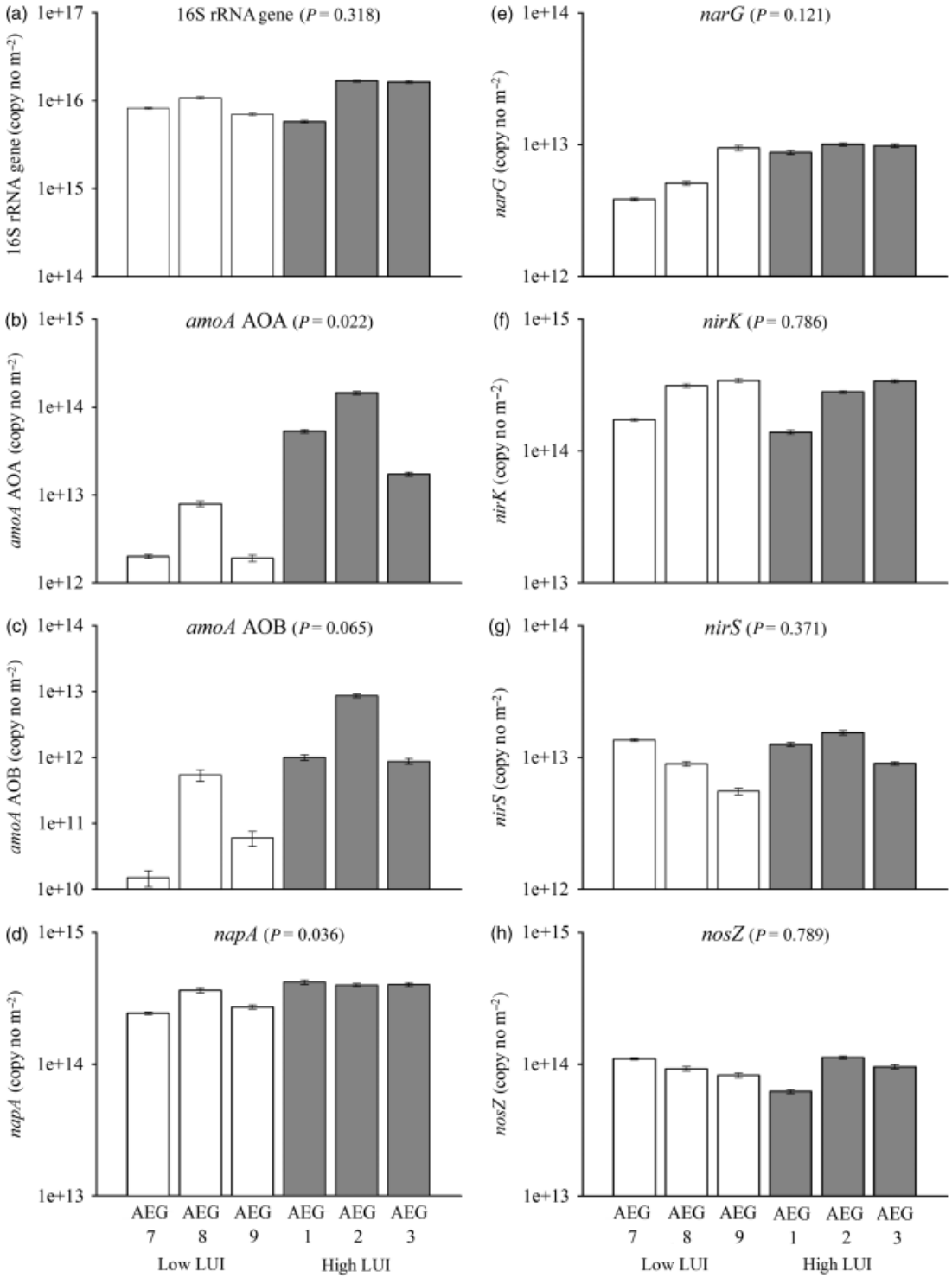

Fig. 1. Average gene copy numbers of total bacterial 16S rRNA genes (a), archaeal (b) and bacterial (c) ammonia oxidizers, nitrate reducers *napA* (d), and *narG* (e) and *nirK*, (f) *nirS* (g) and *nosZ* (h) denitrifiers. Gene copy numbers are expressed per square meter (m^2). Low land-use intensity (LUI) sites are shown in white and high LUI sites are shown in gray graphs. Means ($n = 54$) ± SE. Results of one-way ANOVA for the effects of LUI.

($P = 0.036$) only on *napA* gene abundance, with 8.0×10^{14} and 4.1×10^{14} gene copies m^{-2} in the low and high LUI sites, respectively.

The proportions of the different N-cycling bacterial communities within the total bacterial community expressed as a percentage of a specific gene to 16S rRNA

gene copy numbers did not show significant differences between LUIs (data not shown).

Spatial distribution of biogeochemical properties and N-cycling communities

The results of geostatistical analyses calculated per area are presented in Table 3. For most of the parameters, either the exponential or the spherical spatial model was applied, while C_{org} was best explained by the Gaussian model. The percentage of structural variance indicated that the majority of the data displayed at least moderate spatial dependency at different scales. The full model significantly separated low from high LUI for pH, C_{org}, N_t, NO_3^-, C_{mic}, N_{mic}, C_{mic}/N_{mic} ratio, total bacteria and ammonia oxidizers. For the denitrifying community, the full model best characterized the abundance of *nirS*, while the reduced model provided the best fit for *napA*, *narG*, *nirK* and *nosZ*. Spatial autocorrelations (p-Range) of the different N-cycling communities ranged from 0.31 m for *nosZ* to 159 m for *nirK* (Table 3). In most cases, spatial autocorrelations were within the sampling area (largest possible distance within the grid = 14 m). In general, biogeochemical parameters (pH, C_{org}, N_t and NO_3^-) displayed similar (NO_3^-) or higher spatial autocorrelations in high than in low LUI sites. In contrast, the distribution of the communities studied explained by the full model displayed higher spatial autocorrelations in low LUI. This was reflected by the kriged maps of ammonia oxidizers showing that the distribution of both AOA and AOB was patchier in the high than in the low LUI (Fig. 2). Furthermore, comparison of the kriged maps for AOA and AOB indicated similar distributions of the two groups of ammonia oxidizers in some of the sites. A similar pattern was observed for the spatial distributions of the *napA* and *narG* genes (Fig. 3). The spatial distributions of the highest abundances of *nirK* and *nirS* denitrifiers in low LUI did not overlap (Fig. 4). The maps of *nirS* in high LUI (Fig. 4) as well as of *nosZ* (maps not shown) denitrifiers in both LUIs showed high patchiness, reflecting spatial dependence at a small scale.

Table 3. Results of geostatistical analyses for soil biogeochemical properties and gene copy numbers related to area (m^{-2})

Data	Spatial model	*P*-value (Bonferroni's)	Model used	LUI	Nugget (C_0)	Sill	p-Sill	Structural variance (%)	p-range (m) $P < 0.05$
pH	sph	0.424	Full	Low	0.021	0.117	0.096	82.1	7.50
				High	0.087	0.087	0.07	80.5	23.51
SWC	sph	1	Red	NA	0.104	0.409	0.305	74.6	13.90
C_{org}	gau	0.003	Full	Low	1.16e-18	0.297	0.297	100	0.31
				High	0.448	0.516	0.068	13.2	2.11
N_t	sph	0.122	Full	Low	0.2	0.42	0.220	52.4	0.85
				High	0.544	0.628	0.084	13.4	2.14
NO_3^-	sph	< 0.001	Full	Low	0.889	3.417	2.528	74.0	5.17
				High	47.923	89.539	41.616	46.5	5.03
NH_4^+	sph	1	Red	NA	1.654	NA	1.427	NA	4.77
EOC	exp	1	Red	NA	0.125	NA	0.118	NA	16.06
EN	exp	1	Red	NA	1.904	NA	3.282	NA	8.64
C_{mic}	exp	< 0.001	Full	Low	0.021	0.048	0.027	56.3	82.59
				High	0.062	0.126	0.064	50.8	19.74
N_{mic}	exp	0.002	Full	Low	0.14	0.413	0.273	66.1	159.12
				High	0.222	0.461	0.239	51.8	9.23
C_{mic}/N_{mic}	exp	0.001	Full	Low	0.327	0.386	0.059	15.3	13.69
				High	0.281	0.881	0.6	68.1	3.80
16S	exp	< 0.001	Full	Low	3.112	3.838	0.726	18.9	77.20
				High	6.238	9.36	3.122	33.4	2.77
amoA AOA	sph	< 0.001	Full	Low	0.049	0.075	0.026	34.7	3.95
				High	4.404	9.557	5.153	53.9	1.81
amoA AOB	exp	< 0.001	Full	Low	18.333	22.338	4.005	17.9	7.60
				High	90.485	405.94	314.94	77.7	1.39
napA	sph	1	Red	NA	0.703	NA	0.399	NA	17.31
narG	sph	1	Red	NA	2.804	NA	3.426	NA	9.90
nirK	exp	0.683	Red	NA	0.423	NA	0.894	NA	158.98
nirS	exp	0.007	Full	Low	4.344	11.194	6.850	61.2	50.21
				High	4.711	11.728	7.017	59.8	1.66
nosZ	sph	1	Red	NA	2.916	NA	1.866	NA	0.31

The full model geostatistically separated low from high LUI. No separation between LUI was possible with reduced (red) models.[]NA, not applicable; p-Sill, partial Sill; sph, spherical model; gau, Gaussian model; exp, exponential model.

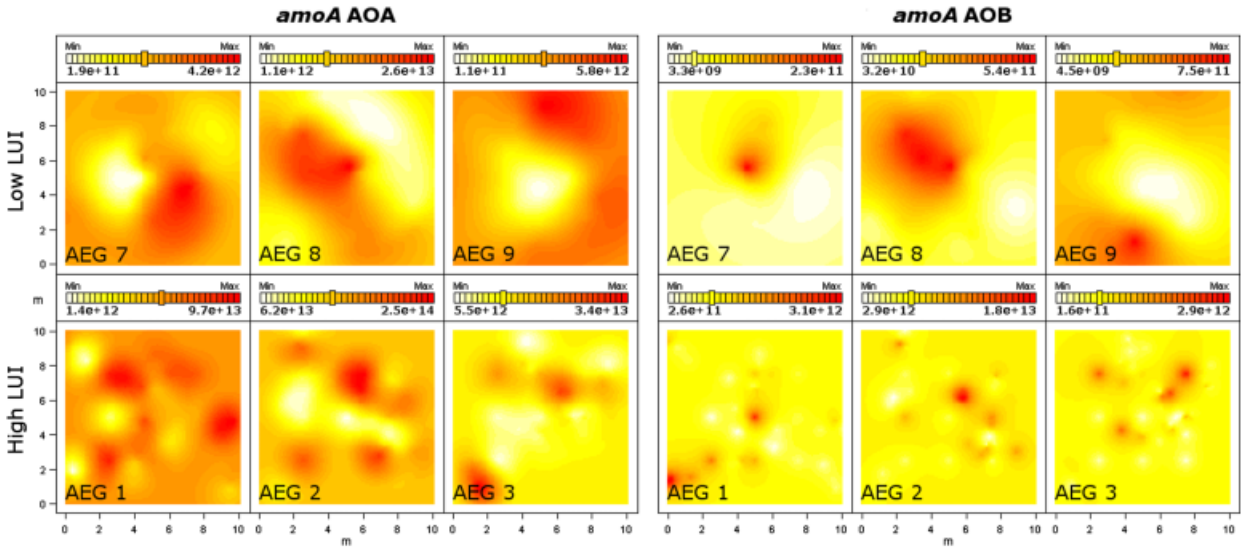

Fig. 2. Kriged maps showing the spatial distribution of ammonia-oxidizing archaea (*amoA* AOA) and bacteria (*amoA* AOB) at the low and high land-use intensity (LUI) grassland sites. Gene copy numbers were related on an area basis (m^{-2}).

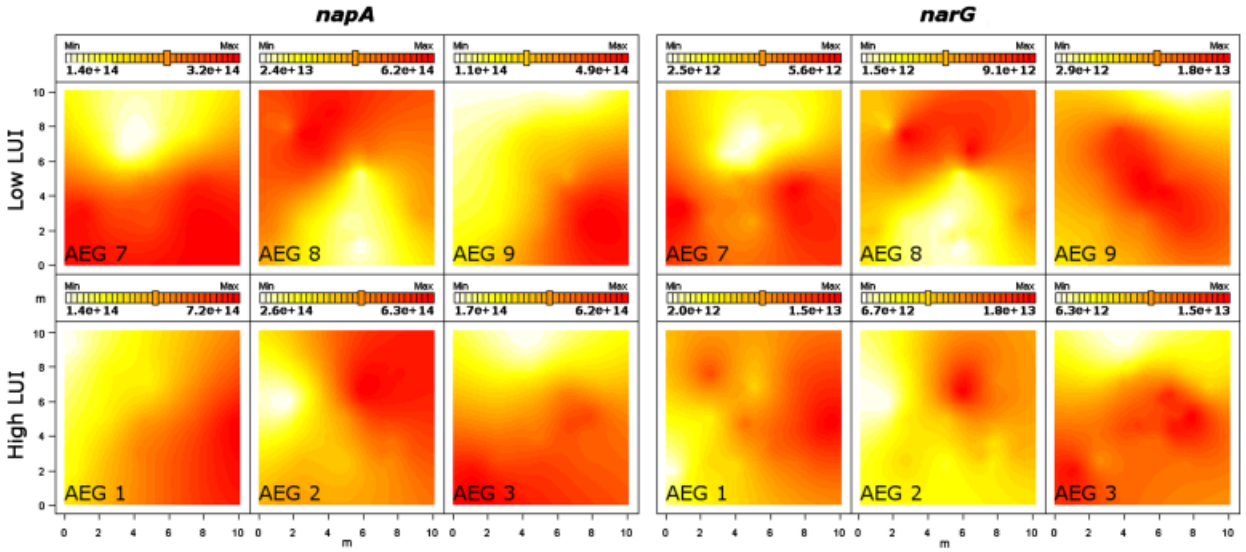

Fig. 3. Kriged maps showing the spatial distribution of *napA* and *narG* nitrate-reducing bacteria at the low and high land-use intensity (LUI) grassland sites. Gene copy numbers were related on an area basis (m^{-2}).

Correlation between biogeochemical soil properties and abundances of ammonia oxidizers and denitrifiers

Spearman correlations were calculated including both LUIs together (Table S3) as well as separately for low (Table S4) and high LUI (Table S5) in order to determine whether different LUIs affect the relationships between parameters. When the two LUIs were considered together, a high correlation (Spearman's correlation $r_s > 0.7$ or $r_s < -0.7$) was observed between the abundance of AOA with the concentration of N_t, AOA with NO_3^-, and of AOB with NO_3^-. The abundances of AOA and AOB were also highly correlated ($r_s = 0.905$) (Table S3). When separately computing Spearman correlations for low and high LUI, correlations between the abundances of ammonia oxidizers and total nitrogen and nitrate concentrations were still evident (Tables S4 and S5). The abundances of both AOA and AOB were also correlated to pH in high (Table S4), but not in low LUI (Table S4). Both AOA ($r_s = 0.738$) and AOB ($r_s = 0.739$) were positively correlated to SWC only in low LUI. In low LUI, *nirK* was negatively correlated with pH and *nirS* was positively correlated. Denitrifiers were positively correlated to N_t (*nirS*) and EN (*nosZ*) only in high LUI (Table S5).

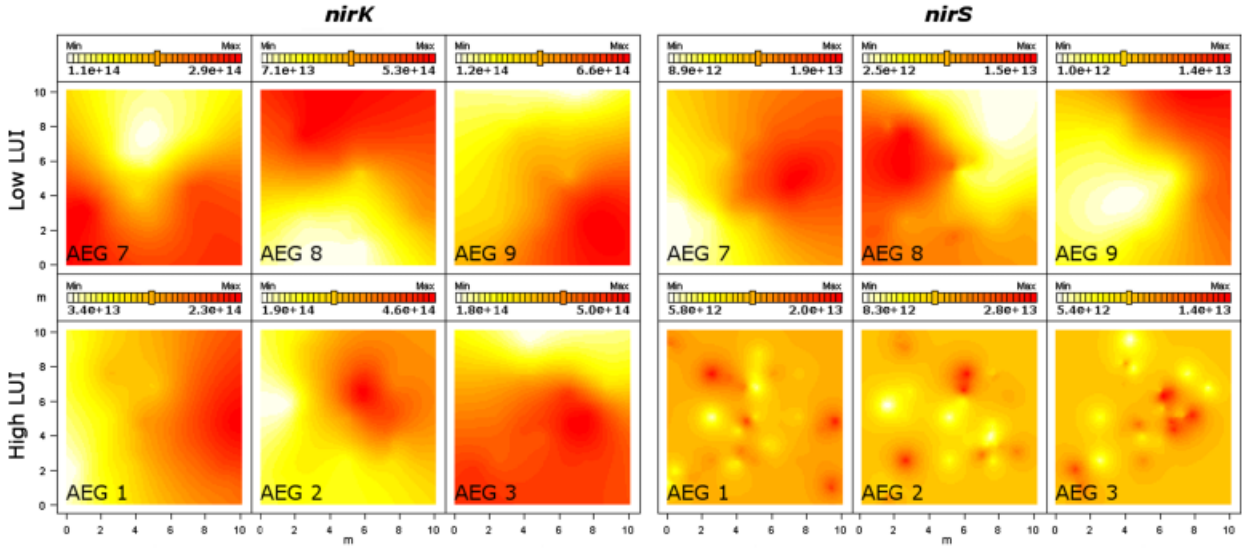

Fig. 4. Kriged maps showing the spatial distribution of *nirK* and *nirS* denitrifying bacteria at the low and high land-use intensity (LUI) grassland sites. Gene copy numbers were related on an area basis (m^{-2}).

Discussion

The sites differed in mowing practices and in whether or not they received fertilizer (Table 1), representing low (unfertilized pastures) and high LUI (fertilized mown meadows) grasslands. The inclusion of three independent sites per LUI enabled us to determine whether LUI significantly affects the spatial patterns of soil biogeochemical properties and of nitrifying and denitrifying microorganisms in soils. Because sites characterized by the same soil type (Rendzic Leptosol) and climatic conditions were selected, management practices were likely the main factor responsible for the differences between treatments.

For most soil biochemical properties, a higher range of spatial autocorrelation, indicated by the p-Range, was observed in the high LUI sites, which indicated reduced spatial heterogeneity. Although bulk density itself did not differ significantly between the two LUIs, both the lowest and the highest bulk densities were found in low LUI sites. Together, these findings support our hypothesis that fertilizer applications and mowing practices at high LUI sites reduced spatial heterogeneity.

Despite high variations between the sites, both archaeal and bacterial ammonia oxidizers were more abundant in the sites of high LUI (Fig. 1 and Table S2). This is in accordance with a study of Hermansson & Lindgren (2001), who reported AOB as being two to three times more abundant in fertilized arable soils than in unfertilized soils. In contrast to soil biogeochemical properties, the ranges of spatial autocorrelation for both AOA and AOB were larger in low than in high LUI sites, resulting in higher patchiness in high LUI sites. In the case of the AOA and AOB, we therefore reject the second part of our hypothesis that high LUI reduces the spatial heterogeneity of soil microorganisms, as results indicated increased spatial heterogeneity at high LUI sites.

Our findings suggest that a combination of factors such as soil structure, microclimate and oxygen status is driving the spatial distribution of AOA and AOB rather than the soil biogeochemical properties investigated.

At the six grassland sites, the average abundance of archaeal ammonia oxidizers was 44 times higher than that of bacterial ammonia oxidizers. Similarly, most studies on ammonia oxidizers in terrestrial ecosystems have reported that AOA were more abundant than AOB (Leininger *et al.*, 2006; He *et al.*, 2007; Nicol *et al.*, 2008). An increasing body of literature has suggested niche partitioning between AOA and AOB, with ammonia concentrations and soil pH as the main environmental factors shaping the ecological niches of ammonia oxidizers (Erguder *et al.*, 2009; Bru *et al.*, 2010; Gubry-Rangin *et al.*, 2010; Schleper, 2010). In the present study, most of the sites investigated showed similar spatial distributions of AOA and AOB (Fig. 2, AEG 2, 3, 8 and 9). This indicated the coexistence of the two groups of ammonia oxidizers, which was further supported by significant positive correlations between the abundances of AOA and AOB (Spearman's $r_s = 0.905$ without separation of LUI). The six grassland sites were characterized by high ammonia concentrations (1.26–3.97 g N m^{-2}) with small variations in pH (6.38–7.09). Because the factors cited above did not separate the niches of AOA and AOB, we suggest that factors, which are otherwise masked by gradients in ammonia concentration or pH, induce the coexistence of the two populations.

The reduction of NO_3^- to NO_2^- can be performed by bacteria harboring either *napA*, *narG* or both genes (Zumft,

1997; Philippot & Højberg, 1999). Only the abundance of the *napA* gene, encoding the periplasmatic nitrate reductase, was significantly higher in high LUI sites. The abundance of the *napA* gene was also one to two orders of magnitude higher than the abundance of *narG*, which encodes the membrane-bound nitrate reductase. This suggests that the abundance of bacteria possessing *napA* may not simply resemble abundances possessing *narG* (Bru *et al.*, 2007), but can be even more abundant under certain conditions. Similar to AOA and AOB, kriged maps showed a similar distribution of the nitrate-reducing microorganisms having the *napA* and *narG* genes (Fig. 3), which was supported by a positive correlation between the two genes (Spearman's $r_s = 0.638$ without separation of LUI). Although the correlation between the two genes was higher in high ($r_s = 0.738$, Table S5) than in low LUI sites ($r_s = 0.524$, Table S4), no differentiation between low and high LUI was possible according to their spatial distribution (reduced model, Table 3). However, it is not possible to determine from our results whether the *napA* and *narG* genes co-occurred in the same organisms or whether bacteria harboring either the *napA* or the *narG* genes coexisted at the studied sites.

Similar to the ammonia oxidizers, the range of spatial autocorrelation for *nirS* was larger in low than in high LUI sites, resulting in a higher patchiness in high LUI sites. In contrast to *nirS*, the distributions of *nirK* and *nosZ* were not affected by LUI. The different spatial distributions of *nirK*- and *nirS*-type denitrifiers (Fig. 4), together with the negative correlation between the abundances of *nirK* and *nirS* (Spearman's $r_s = -0.356$), indicate a niche differentiation of organisms having the *nirK* and *nirS* functional genes in low LUI sites. The nitrite reductases encoded by *nirK* and *nirS* are functionally homologous (Glockner *et al.*, 1993) and no denitrifying organism harboring both types of nitrite reductases has been reported as yet (Jones *et al.*, 2008). Previous studies (Hallin *et al.*, 2009; Philippot *et al.*, 2009b; Enwall *et al.*, 2010) have discussed the maintenance of two types of nitrite reductases as a result of niche differentiation, thus avoiding competitive exclusion. Furthermore, Hallin *et al.* (2009) discussed the distribution patterns among *nirK*- and *nirS*-type denitrifiers through habitats created by the absence/presence of plants, and both Enwall *et al.* (2010) and Bru *et al.* (2010) reported copper as being a strong driver for *nirK*-type denitrifiers.

Spatial analysis of microbial habitat characteristics and soil microbial communities is a powerful tool to understand not only links between environmental drivers and microbial abundance but also to reveal coexistence or niche partitioning of soil microorganisms. Whereas these links are well established in distinct microhabitats (e.g. rhizo- and detritusphere) (Haase *et al.*, 2008; Poll *et al.*, 2008), our study is one of the first to show that grassland management (e.g. LUI) differentially changes spatial patterns of soil biogeochemical properties and N-cycling microorganisms at the plot scale. Spatial heterogeneity decreased with higher LUI for biogeochemical properties, but increased for N-cycling microorganisms, indicating that spatially structured abiotic or biotic factors that were not taken into account are driving the microbial distribution in our study. Independent of LUI, we also found similar spatial distributions of the bacterial and archaeal ammonia oxidizers, while contrasting distributions were observed for *nirS* and *nirK* denitrifiers. This suggests that niche partitioning occurred only between the denitrifiers harboring either the copper or the cd_1 heme nitrite reductase. Because LUI also changes plant community composition and diversity, future studies will have to evaluate the impact of different plant species and the quality of their rhizodeposits on the spatial distribution of N-cycling microorganisms.

Acknowledgements

The work has been funded by the DFG Priority Program 1374 'Infrastructure-Biodiversity-Exploratories' (KA 1590/8-1). Field work permits were given by the responsible state environmental offices of Baden-Württemberg. We thank Kathleen Regan for English spelling corrections.

References

Bardgett RD & Wardle DA (2003) Herbivore-mediated linkages between aboveground and belowground communities. *Ecology* **84**: 2258–2268.

Becker JM, Parkin T, Nakatsu CH, Wilbur JD & Konopka A (2006) Bacterial activity, community structure, and centimeter-scale spatial heterogeneity in contaminated soil. *Microb Ecol* **51**: 220–231.

Bolton H Jr, Wildung RE & Smith JL (1990) Nitrogen mineralization potentials of shrub-steppe soils with different disturbance histories. *Soil Sci Soc Am J* **54**: 887–891.

Bolton H Jr, Smith JL & Link SO (1993) Soil microbial biomass and activity of a disturbed and undisturbed shrub-steppe ecosystem. *Soil Biol Biochem* **25**: 545–552.

Bremer C, Braker G, Matthies D, Reuter A, Engels C & Conrad R (2007) Impact of plant functional group, plant species, and sampling time on the composition of *nirK*-type denitrifier communities in soil. *Appl Environ Microb* **73**: 6878–6884.

Bru D, Sarr A & Philippot L (2007) Relative abundances of proteobacterial membrane-bound and periplasmic nitrate reductases in selected environments. *Appl Environ Microb* **73**: 5971–5974.

Bru D, Ramette A, Saby NPA, Dequiedt S, Ranjard L, Jolivet C, Arrouays D & Philippot L (2010) Determinants of the distribution of nitrogen-cycling microbial communities at the landscape scale. *ISME J* **5**: 532–542.

Cambardella CA, Moorman TB, Parkin TB, Karlen DL, Novak JM, Turco RF & Konopka AE (1994) Field-scale variability of

soil properties in central Iowa soils. *Soil Sci Soc Am J* **58**: 1501–1511.

Doran JW & Parkin TB (1996) Quantitative indicators of soil quality: a minimum data set. *Methods for Assessing Soil Quality. Soil Science Society American Special Publications No. 49*, pp. 25–37.

Enwall K, Throbäck IN, Stenberg M, Söderström M & Hallin S (2010) Soil resources influence spatial patterns of denitrifying communities at scales compatible with land management. *Appl Environ Microb* **76**: 2243–2250.

Erguder TH, Boon N, Wittebolle L, Marzorati M & Verstraete W (2009) Environmental factors shaping the ecological niches of ammonia oxidizing archaea. *FEMS Microbiol Rev* **33**: 855–869.

Ettema CH & Wardle DA (2002) Spatial soil ecology. *Trends Ecol Evol* **17**: 177–183.

Fierer N & Jackson RB (2006) The diversity and biogeography of soil bacterial communities. *P Natl Acad Sci USA* **103**: 626–623.

Fischer M, Bossdorf O, Gockel S *et al.* (2010) Implementing large-scale and long-term functional biodiversity research: the Biodiversity Exploratories. *Basic Appl Ecol* **11**: 473–485.

Frank DA & Groffmann PM (1998) Ungulate vs. landscape control of soil C and N processes in grasslands of Yellowstone National Park. *Ecology* **79**: 2229–2241.

Franklin RB & Mills AL (2003) Multi-scale variation in spatial heterogeneity for microbial community structure in an eastern Virginia agricultural field. *FEMS Microbiol Ecol* **44**: 335–346.

Glockner AB, Jüngst A & Zumft WG (1993) Copper-containing nitrite reductase from *Pseudomonas aureofaciens* is functional in a mutationally cytochrome cd_1-free background (NirS-) of *Pseudomonas stutzeri*. *Arch Microbiol* **160**: 18–26.

Grundmann G & Debouzie D (2000) Geostatistical analysis of the distribution of NH_4^+ and NO_2^--oxidizing bacteria and serotypes at the millimeter scale along a soil transect. *FEMS Microbiol Ecol* **34**: 57–62.

Gubry-Rangin C, Nicol GW & Prosser J (2010) Archaea rather than bacteria control nitrification in two agricultural acidic soils. *FEMS Microbiol Ecol* **74**: 566–574.

Haase S, Philippot L, Neumann G, Marhan S & Kandeler E (2008) Local response of bacterial densities and enzyme activities to elevated atmospheric CO_2 and different N supply in the rhizosphere of *Phaseolus vulgaris* L. *Soil Biol Biochem* **40**: 1225–1234.

Hallin S, Jones CM, Schloter M & Philippot L (2009) Relationship between N-cycling communities and ecosystem functioning in a 50-year-old fertilization experiment. *ISME J* **3**: 597–605.

He J, Shen J, Zhang L, Zhu Y, Zheng Y, Xu M & Di H (2007) Quantitative analyses of the abundance and composition of ammonia-oxidizing bacteria and ammonia-oxidizing archaea of a Chinese upland red soil under long-term fertilization practices. *Environ Microbiol* **9**: 2364–2374.

Henry S, Baudoin E, López-Gutiérrez JC, Martin-Laurent F, Brauman A & Philippot L (2004) Quantification of denitrifying bacteria in soils by *nirK* gene targeted real-time PCR. *J Microbiol Meth* **59**: 327–335 Corrigendum in *J Microbiol Meth* **6** (2005): 289–290.

Henry S, Bru D, Stres B, Hallet S & Philippot L (2006) Quantitative detection of the *nosZ* gene, encoding nitrous oxide reductase, and comparison of the abundances of 16S rRNA, *narG*, *nirK*, and *nosZ* genes in soils. *Appl Environ Microb* **72**: 5181–5189.

Hermansson A & Lindgren P-E (2001) Quantification of ammonia-oxidizing bacteria in arable soil by real-time PCR. *Appl Environ Microb* **67**: 972–976.

Isaaks EH & Srivastava RM (1989) *An Introduction to Applied Geostatistics*. Oxford University Press, New York.

Joergensen RG (1996) The fumigation-extraction method to estimate soil microbial biomass: Calibration of the KEC value. *Soil Biol Biochem* **28**: 25–31.

Joergensen RG & Müller T (1996) The fumigation-extraction method to estimate soil microbial biomass: Calibration of the KEN value. *Soil Biol Biochem* **28**: 33–37.

Jones CM, Stres B, Rosenquist M & Hallin S (2008) Phylogenetic analysis of nitrite, nitric oxide, and nitrous oxide respiratory enzymes reveal a complex evolutionary history for denitrification. *Mol Biol Evol* **25**: 1955–1966.

Kandeler E, Deiglmayr K, Tscherko D, Bru D & Philippot L (2006) Abundance of *narG*, *nirS*, *nirK*, and *nosZ* genes of denitrifying bacteria during primary successions of a glacier foreland. *Appl Environ Microb* **72**: 5957–5962.

Leininger S, Urich T, Schloter M, Schwark L, Qi J, Nicol GW, Prosser JI, Schuster SC & Schleper C (2006) Archaea predominate among ammonia-oxidizing prokaryotes in soils. *Nature* **442**: 806–809.

Le Roux X, Bardy M, Loiseau P & Louault F (2003) Stimulation of soil nitrification and denitrification by grazing in grasslands: do changes in plant species composition matter? *Oecologia* **137**: 417–425.

López-Gutiérrez JC, Henry S, Hallet S, Martin-Laurent F, Catroux G & Philippot L (2004) Quantification of a novel group of nitrate-reducing bacteria in the environment by real-time PCR. *J Microbiol Meth* **57**: 399–407.

Meyer A, Radl V, Keil D, Welzl G, Schöning I, Boch S, Marhan S, Kandeler E, Munch JC & Schloter M (2010) Different land use intensities in grassland ecosystems drive ecology of microbial communities involved in nitrogen turnover in soil. *Environ Microbiol Rep*, under revision.

Miller MN, Zebarth BJ, Dandie CE, Burton DL, Goyer C & Trevors JT (2009) Denitrifier community dynamics in soil aggregates under permanent grassland and arable cropping systems. *Soil Sci Soc Am J* **73**: 1843–1851.

Nicol GW, Leininger S, Schleper C & Prosser JI (2008) The influence of soil pH on the diversity, abundance and transcriptional activity of ammonia oxidizing archaea and bacteria. *Environ Microbiol* **10**: 2966–2978.

Niklaus PA, Wardle DA & Tate KR (2006) Effects of plant species diversity and composition on nitrogen cycling and the trace gas balance of soils. *Plant Soil* **282**: 83–98.

Patra AK, Abbadie L, Clays-Josserand A *et al.* (2005) Effects of grazing on microbial functional groups involved in soil N dynamics. *Ecol Monogr* **75**: 65–80.
Philippot L (2002) Denitrifying genes in bacterial and archaeal genomes. *BBA-Gene Struct Expr* **1577**: 355–376.
Philippot L & Højberg O (1999) Dissimilatory nitrate reductases in bacteria. *Biochim Biophys Acta* **1446**: 1–23.
Philippot L, Hallin S & Schloter M (2007) Ecology of denitrifying prokaryotes in agricultural soil. *Adv Agron* **96**: 249–305.
Philippot L, Bru D, Saby NP, Cuhel J, Arrouays D, Šimek M & Hallin S (2009a) Spatial patterns of bacterial taxa in nature reflect ecological traits of deep branches of the 16S rRNA bacterial tree. *Environ Microbiol* **11**: 3096–3104.
Philippot L, Cuhel J, Saby NP, Chèneby D, Chronáková A, Bru D, Arrouays D, Martin-Laurent F & Šimek M (2009b) Mapping field-scale spatial patterns of size and activity of the denitrifier community. *Environ Microbiol* **11**: 1518–1526.
Poll C, Marhan S, Ingwersen J & Kandeler E (2008) Dynamics of litter carbon turnover and microbial abundance in a rye detritusphere. *Soil Biol Biochem* **40**: 1306–1321.
R Development Core Team (2008) *R: A language and environment for statistical computing*. R Foundation for Statistical Computing, Vienna, Austria. Available at http://www.R-project.org.
Ritz K, McNicol J, Nunan N *et al.* (2004) Spatial structure in soil chemical and microbiological properties in an upland grassland. *FEMS Microbiol Ecol* **49**: 191–205.
Robinson GK (1991) That BLUP is a good thing: the estimation of random effects. *Stat Sci* **6**: 15–32.
Rotthauwe J, Witzel K & Liesack W (1997) The ammonia monooxygenase structural gene *amoA* as a functional marker: molecular fine-scale analysis of natural ammonia-oxidizing populations. *Appl Environ Microb* **63**: 4704–4712.
SAS Institute Inc. (1999) *SAS/STAT® User's Guide, Version 9.2*. SAS Institute Inc, Cary, NC.
Schabenberger O & Pierce FJ (2002) *Contemporary Statistical Models for the Plant and Soil Sciences*. CRC Press, Boca Raton.
Schleper C (2010) Ammonia oxidation: different niches for archaea and bacteria? *ISME J* **4**: 1092–1094.
Tiedje J, Simkins S & Groffman P (1989) Perspectives on measurement of denitrification in the field including recommended protocols for acetylene based methods. *Plant Soil* **115**: 261–284.
Treusch AH, Leininger S, Kletzin A, Schuster SC, Klenk HP & Schleper C (2005) Novel genes for nitrite reductase and Amo-related proteins indicate a role of uncultivated mesophilic crenarchaeota in nitrogen cycling. *Environ Microbiol* **7**: 1985–1995.
Vance ED, Brookes PC & Jenkinson DS (1987) An extraction method for measuring soil microbial biomass C. *Soil Biol Biochem* **19**: 703–707.
Zumft W (1997) Cell biology and molecular basis of denitrification. *Microbiol Mol Biol R* **61**: 533–616.

Supporting Information

Additional Supporting Information may be found in the online version of this article:

Fig. S1. Schematic of sampling design.
Table S1. Biogeochemical soil properties.
Table S2. Average gene copy numbers for each grassland site expressed per gram dry soil.
Table S3. Spearman correlations between soil biogeochemical parameters and gene abundances related to area (m^{-2}) without separation of LUI.
Table S4. Spearman correlations between soil biogeochemical parameters and gene abundances related to area (m^{-2}) in low LUI.
Table S5. Spearman correlations between soil biogeochemical parameters and gene abundances related to area (m^{-2}) in high LUI.

Please note: Wiley-Blackwell is not responsible for the content or functionality of any supporting materials supplied by the authors. Any queries (other than missing material) should be directed to the corresponding author for the article.